Vol. 47, No. 1 (2025) 125-136, DOI: 10.24874/ti.1863.01.25.03

Tribology in Industry

www.tribology.rs

RESEARCH

Optimizing Bioceramic Composites for Hip Joint Replacements using SPS Method: Investigating the Effects of Titanium Diboride (TiB_2) on Tribological Properties

Pavankumar Ravikumar[a,*], Goud Mallesh[b], S. Suresh Kumar[c], H. S. Manjunatha[a]

[a]*Department of Mechanical Engineering, SJCE, JSS Science and Technology University, Mysore, India*
[b]*Department of Mechanical Engineering, Sri Jayachamarajendra College Engineering, JSS S&T University, Mysore, India,*
[c]*Department of Mechanical Engineering, The National institute of Engineering, Mysore, India.*

Keywords:

Hip implant
Bioceramic composites
L27 orthogonal array
Pin on disk
Wear test

* Corresponding author:

Pavankumar Ravikumar
E-mail: pavanjce2016@gmail.com

Received: 6 January 2025
Revised: 17 February 2025
Accepted: 11 March 2025

A B S T R A C T

This study investigates the fabrication, characterization, and tribological behavior of bioceramic composites specifically engineered for hip joint replacements. Utilizing the Spark Plasma Sintering (SPS) process, advanced ceramic composites were developed, comprising alumina (Al_2O_3), silicon carbide (SiC), magnesium oxide (MgO), and titanium diboride (TiB_2) integrated with an Al6061 base. The objective was to enhance mechanical strength, wear resistance, and biocompatibility for long-term orthopedic applications.

Material characterization was performed using Energy Dispersive X-ray Spectroscopy (EDS) and X-ray Diffraction (XRD) techniques, confirming the presence of reinforcing phases and crystalline structures. Wear tests were conducted using a pin-on-disk apparatus, and wear losses were systematically evaluated using a Design of Experiments (DOE) approach with an L27 orthogonal array. Statistical analysis using Minitab software revealed significant differences in tribological performance among composites with varying TiB_2 concentrations. Notably, the weight percentage of reinforcement was identified as the most influential factor on wear loss (p-value = 0.000), with higher TiB_2 percentages correlating with improved mechanical performance. The optimal composition—5% alumina, 5% SiC, 2% MgO, and 9% TiB_2 combined with Al6061—demonstrated enhanced toughness and fracture resistance while addressing the fragility commonly associated with ceramic materials. The model fit was confirmed by an R-squared value of 89.21%, indicating strong predictive capability. SEM analysis post-wear testing highlighted reduced wear tracks in TiB_2-reinforced samples. These findings suggest that bioceramic composites exhibit durability against wear, friction, and fracture resistance, which are critical for the long-term effectiveness of hip implants. The study provides a foundation for further investigations into advanced mechanical testing, biocompatibility assessments, and clinical relevance to ensure suitability for orthopedic applications.

1. INTRODUCTION

Bioceramic materials have gained significant popularity in modern Orthopaedics due to their unique properties, including corrosion resistance, biocompatibility, and wear endurance. These characteristics make them particularly effective in medical applications, especially in hip joint surgeries [1].

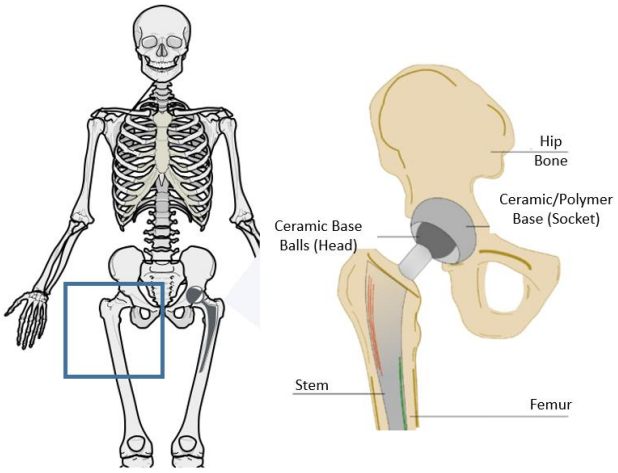

Fig. 1. Hip joint and hip implant.

Total Hip Arthroplasty (THA) is a surgical procedure that replaces damaged components of the hip joint with artificial implants. Traditionally, metal and polymer components have been the materials of choice for hip replacements due to their ease of manufacturing and availability [2]. However, these metal and polymer-based implants often encounter issues related to wear, leading to complications such as inflammation, discomfort, loosening of the implants, and the accumulation of wear particles. Over time, this accumulation can result in osteolysis and bone depletion, posing significant challenges for long-term recovery and functionality. Ultimately, these complications can lead to the breakdown of the implant.

The introduction of bioceramics has significantly transformed the field of biomaterials by effectively addressing the limitations associated with traditional materials. Advances in hip joint replacement technologies have resulted in more durable implants, enabling patients to regain mobility and independence following surgery [3].

Common bioceramics used in hip implant surgery include alumina (Al_2O_3), zirconia (ZrO_2), silicon carbide (SiC), calcium oxide (MgO), hydroxyapatite (HA), tricalcium phosphate (TCP), and biphasic calcium phosphate (BCP). These materials are often combined or incorporated with metals or polymers to produce customized implants. Bioceramics are typically utilized in fabricating the implant's head and socket (Figure 2) [4].

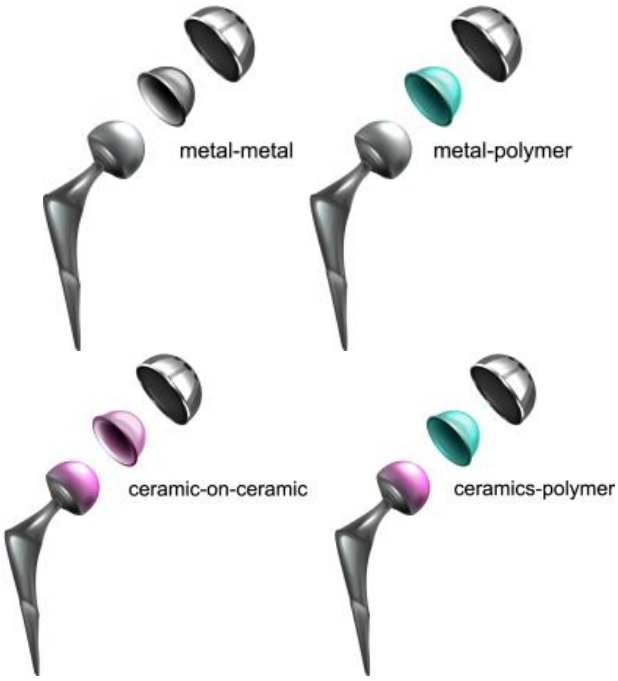

Fig. 2. Hip implant material combinations. Current experiment involves metal and ceramic composites [6].

In the current research, advanced bioceramic composites were fabricated with varying weight percentages of alumina, titanium diboride (TiB_2), silicon carbide (SiC), magnesium oxide (MgO), and Al6061 using the Spark Plasma Sintering (SPS) process. The fabricated composites were subjected to wear testing using a pin-on-disk apparatus, employing an L27 orthogonal array to evaluate wear loss concerning weight percentage, sliding distance, speed, and load parameters [5].

2. MATERIAL AND METHODS

The primary objective of this study was to select and evaluate bioceramics for use in hip joint implants. Ceramic-based implants are distinguished from Biometals by their exceptional properties, including superior wear resistance, corrosion resistance, and compatibility with biological systems, which enhance their efficacy in medical applications.

Among the materials selected for the fabrication of composites, alumina (Al_2O_3) stands out due to its remarkable hardness (90 GPa) and chemical stability, along with a low friction coefficient of 0.05 [7]. The addition of silicon carbide (SiC) further enhances wear resistance, offering impressive strength (450 MPa) and stiffness (450 GPa), with a friction coefficient of 0.1. Magnesium oxide (MgO) serves as an effective filler material, characterized by a low friction coefficient (0.1), a high melting point (280°C), and excellent biocompatibility [8]. Titanium diboride (TiB_2) is notable for its exceptional hardness (28-30 GPa), high-temperature resistance (melting point: 2930°C), and excellent wear resistance, making it an attractive reinforcement phase in bioceramic composites. Additionally, TiB_2 exhibits good biocompatibility, corrosion resistance, and bioinertness, with a density of 4.52 g/cm^3 and a Young's modulus of 530-570 GPa, rendering it suitable for biomedical applications. Aluminum alloy Al6061 is also an excellent choice for hip implants due to its high stiffness (70 GPa), high strength (290 MPa), biocompatibility, and corrosion resistance [9].

The optimal performance of hip joint implants in minimizing wear and friction between moving components is crucial for their longevity and to reduce the likelihood of future surgical interventions. The primary goal of studying tribology is to understand how bioceramic materials interact with each other and with natural body fluids, such as synovial fluid, which naturally lubricates joints [10,11]. The enhanced surface characteristics of bioceramics, including durability and smoothness, contribute to reduced wear and strain over time, offering numerous benefits. However, it is important to note that bioceramics can be susceptible to brittleness, which may lead to abrupt failure under substantial pressures.

In this experiment, nine sample combinations were prepared with varying compositions of TiB_2, alumina, MgO, and SiC to assess the advantages and disadvantages of TiB_2. The specimens were fabricated with three distinct TiB_2 concentrations (3%, 6%, and 9%) to investigate their collective influence on wear properties. This systematic approach allows for a comprehensive understanding of the impact of TiB_2, ranging from minimal to maximal concentrations.

Magnesium Powder
Elastic modulus: 41–45 GPa. Density - 1.74 g/cm^3
High biocompatibility; promotes bone growth and osteoblast differentiation.

Boron Carbide
V. hardness: 38 GPa
Density -2.4 g/cm^3
Not typically biocompatible; used for wear resistance and shielding applications.

Al 6061 Sticks
Tensile strength: 310 MPa
Density - 2.6 g/cm^3. Good corrosion resistance; widely used in biomedical devices.

Titanium Di-Boride
Surface hardness: 296.3 kg/mm^2. 4.52 g/cm^3. Needs further investigation for biocompatibility.

Silicon Carbide Powder
Mohs hardness: ~9.5~3.21 g/cm^3
High wear resistance and thermal stability; not inherently biocompatible but used in composites for durability.

Fig. 3. Materials used for fabrication.

The combined effect of adding silicon carbide (SiC) and alumina (Al_2O_3) significantly enhances the durability of the composite material. The strong and rigid nature of silicon carbide contributes to the overall properties, while alumina's high hardness and stiffness provide excellent wear resistance [12]. The amalgamation of these two components yields an exceptional composite well-suited for use in hip arthroplasty.

A uniform weight fraction of 2% magnesium oxide (MgO) was employed as a sintering aid in the fabrication of bioceramic composites. MgO plays a critical role in the sintering process by reducing the sintering temperature, improving the densification of the ceramic matrix, and enhancing the mechanical properties of the final composite. Additionally, MgO is recognized for its excellent biocompatibility, which is essential for biomedical applications. By maintaining a consistent MgO content, variations in the composite properties can be primarily attributed to differences in the other constituents, namely alumina (Al_2O_3), silicon carbide (SiC), titanium diboride (TiB_2), and aluminum alloy (Al6061).

Bioceramic composites can be manufactured using several conventional methods, including pressure-less sintering, hot pressing, and conventional sintering. However, these methods often result in significant grain expansion and porosity, typically requiring lengthy processing times and high temperatures.

In contrast, spark plasma sintering (SPS) offers several advantages, including reduced sintering time, the production of finer-grained microstructures, and enhanced mechanical characteristics. SPS achieves this by rapidly densifying the powder mixture using high pressure and pulsed electric current [13]. Furthermore, SPS allows for more precise control over the sintering process, enabling the production of complex ceramic composites with tailored properties. The SPS method necessitates several essential processes to ensure the ideal microstructure and strength of the composites [14].

Table 1.

Materials	Weight fraction (%)								
	S_1	S_2	S_3	S_4	S_5	S_6	S_7	S_8	S_9
Alumina (Al_2O_3)	10	0	5	10	0	5	10	0	5
Silicon carbide (SiC)	0	10	5	0	10	5	0	10	5
Magnesium Oxide (MgO)	2	2	2	2	2	2	2	2	2
TiB_2	3	3	3	6	6	6	9	9	9
Aluminium (Al6061)	88	88	88	86	86	86	84	84	84

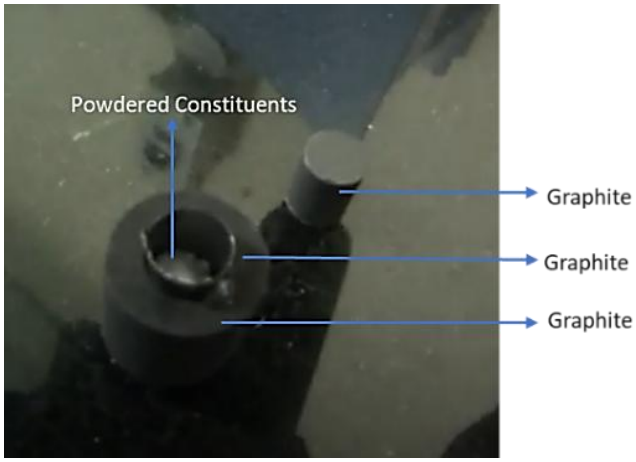

Step I. Powder Poured into Die

Step II. Die Placement in SPS machine

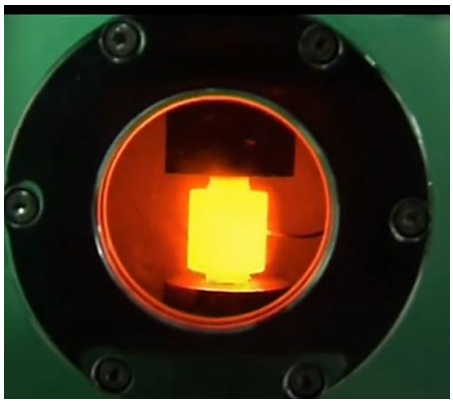

Step III. Red Hot stage in the SPS machine (1400°C)

Step IV. Final Die

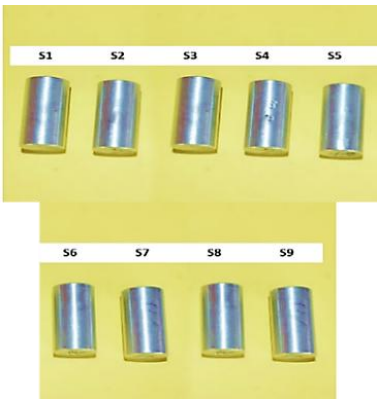

Final Specimens

Fig. 4. Fabrication process.

2.1 Fabrication process

The Spark Plasma Sintering (SPS) process is an advanced powder metallurgy technique that uses pulsed DC current to generate localized heating at particle interfaces, enabling rapid densification with minimal grain growth. This method is highly effective in producing composites with enhanced mechanical properties, wear resistance, and uniform microstructures, making it ideal for high-performance applications like bioceramic composites.

Powder preparation: The powder preparation and mixing process involves milling all components—aluminum alloy (Al6061), titanium diboride (TiB_2), silicon carbide (SiC), magnesium oxide (MgO), and alumina (Al_2O_3). Since all materials, except for Al6061, are already in powder form, the Al6061 sticks are first converted into a fine powder using the grinder. The grinding is performed under controlled conditions to ensure uniform particle size distribution, which is critical for achieving homogeneity in the composite. After milling, the powder mixture is filtered using a fine mesh sieve and dried in an oven at 100°C to eliminate moisture and ensure consistent particle size and distribution.

Moulding and die placement: To facilitate easy removal, the dry powder mixture is pressed into a graphite die using graphitic paper and plunges. The graphite die is specifically chosen for its ability to withstand high temperatures during sintering while preventing contamination of the composite. The graphitic paper acts as a separator to avoid adhesion between the die walls and the composite material during pressing.

Sintering conditions: The Spark Plasma Sintering (SPS) process is conducted using a state-of-the-art SPS system equipped with precise temperature and pressure controls. The sintering process is conducted under 60 MPa of pressure, with a rapid temperature rise to 1400°C, followed by a 3-minute holding period to ensure proper densification. During sintering, pulsed DC current is applied to generate localized heating at particle interfaces, promoting rapid densification while minimizing grain growth. This method ensures high mechanical strength and improved wear resistance in the final product.

Final product: The resulting cylindrical models (10 mm diameter and 30 mm length) are designed for testing, particularly for the pin-on-disk experiment. These models exhibit increased densification, high mechanical strength, reduced grain formation, and improved wear resistance. The uniform distribution of reinforcing phases ensures consistent tribological performance across specimens. A total of nine different specimens were fabricated with varying combinations of constituents (S1 to S9) to be subjected to tests.

2.2 Wear analysis and optimization

To verify the compatibility of the composite with the testing apparatus, the hardness of the composites was evaluated. Based on the results obtained, the disc utilized for the wear test was chosen. Consequently, an EN31 hardened steel disc, exhibiting a hardness of 62 Rockwell (HRC) and a diameter of 180 millimeters, was selected for all samples. (Figure 5). The details of

experimental design is explained in next section [9]. Experimental Design - The levels for each parameter in Table 2 and the L27 orthogonal array were carefully selected to ensure a systematic and efficient investigation of the tribological behavior of Al6061-TiB_2 composites.

Weight % of Reinforcement (3%, 6%, 9%): These levels were chosen to evaluate the effect of increasing TiB_2 content on wear resistance and mechanical properties. Lower percentages provide baseline data, while higher percentages test the composite's limits without inducing brittleness.

Speed (2 m/s, 3 m/s, 4 m/s): This range simulates realistic sliding conditions relevant to hip joint applications. Speeds below 2 m/s may not induce significant wear, while speeds above 4 m/s could exceed practical operational limits.

Load (10 N, 20 N, 30 N): These loads represent typical forces experienced in hip joints during activities ranging from walking to running, ensuring physiological relevance.

Distance (1000 m, 2000 m, 3000 m): These distances simulate extended wear cycles to assess long-term durability under various conditions.

The L27 orthogonal array was selected due to its ability to efficiently study four parameters at three levels each with minimal experimental runs (27 tests). This design balances resource constraints with comprehensive data coverage, enabling robust statistical analysis through ANOVA and Signal-to-Noise ratio calculations. The approach ensures meaningful insights into parameter interactions while minimizing experimental effort.

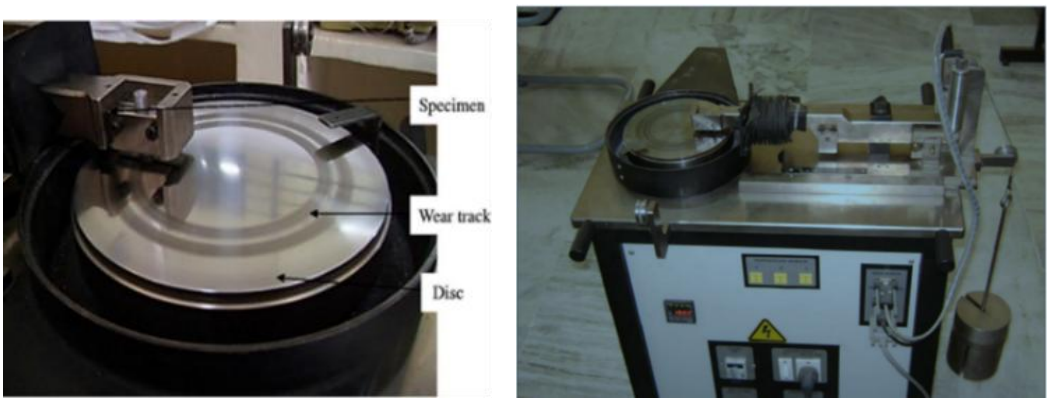

Fig 5. Pin on disk setup Test parameters: Load = 10 N to 30 N, Speed = 2 m/s to 4 m/s, Distance = 1000 - 3000 m. The wear loss was measured after each test.

Table 2. Experimental design

Parameter	Level 1	Level 2	Level 3
Weight % of Reinforcement	3	6	9
Speed (m/s)	2	3	4
Load (N)	10	20	30
Distance (M)	1000	2000	3000

3. RESULT AND DISCUSSION

Characterization of bioceramic composites using EDX and XRD

In the development of bioceramic composites for hip joint replacements, EDX and XRD are employed to characterize the material's composition, structure, and properties. These results analyze the elemental composition of the composite material, confirming the presence of alumina (Al_2O_3), silicon carbide (SiC), magnesium oxide (MgO), and titanium diboride (TiB_2).

3.1 Energy Dispersive Spectrum (EDS)

EDS is an analytical technique that identifies a specimen's elemental composition using X-ray spectra.

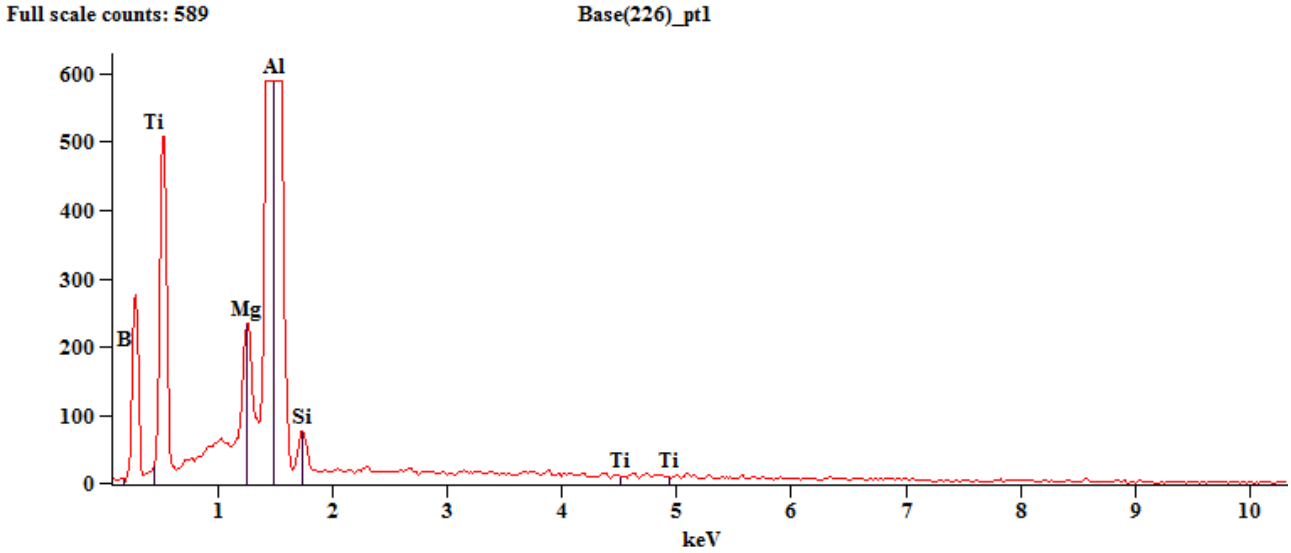

Fig 6. EDS analysis results from 9% TiB_2 sample.

In this study, EDS analysis was performed on composites with varying TiB_2 weight percentages to determine their elemental composition. The resulting spectra reveal that aluminium exhibits high-intensity peaks, indicating its predominance as the base alloy. Additionally, the presence of titanium, magnesium, boron, and silicon elements is confirmed by their low-intensity peaks, which correspond to the reinforcing phases (Figure 6).

3.2 X ray diffraction (XRD)

XRD patterns of the composites were obtained using a Panalytical X-ray diffractometer. The patterns confirm the formation of TiB_2 particles in the composites. The crystalline size measurements were carried out using Debye-Scherrer equation.

$$D_{hkl} = \frac{0.98\lambda}{\beta \cos\theta} \quad (1)$$

The XRD pattern of the 9% TiB_2 sample (Figure 7) shows characteristic peaks consistent with JCPDS files No. 89-2837 and 4-829. The intensity of TiB_2 is highest in the (1 0 1) plane (2θ = 44.6714°, JCPDS 07-0275). Aluminium peaks are prominent, notably at 2θ=38.7618°, 65.3376°, 78.4779° of (1 1 0), (2 0 0), (3 1 1) of the diffraction peak of Al6061, corresponding to file No. 89-2837. TiB_2 peaks are minor, at 2θ angle 45.0223°, 61.3770°, 78.3867° of (1 0 1), (1 1 0), (2 0 1) of the diffraction peaks of TiB_2, corresponding to file No. 07-0275.

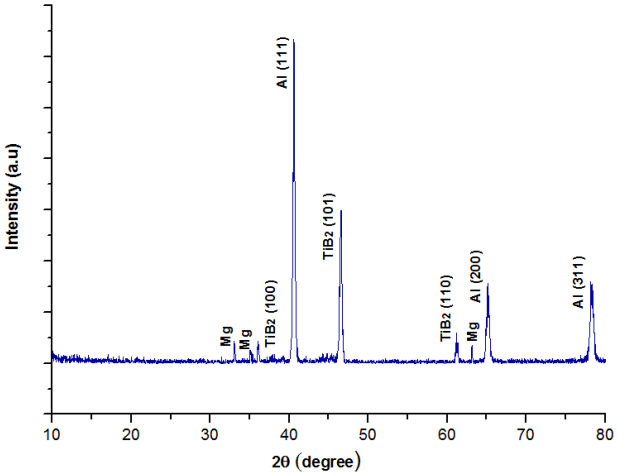

Fig 7. XRD pattern results from 9% TiB_2 sample.

Table 3. Identified peaks and corresponding phases for different materials.

2θ (degrees)	Phase	JCPDS File No.
38.76	Al6061 (110)	89-2837
44.67	TiB_2 (101)	07-0275
65.33	Al6061 (200)	89-2837
45.02	TiB_2 (110)	07-0275
61.37	TiB_2 (201)	07-0275
78.f39	TiB_2 (210)	07-0275

3.3 Wear test results

Using Pin on disk, Bio-ceramic composites with varying weight fractions of Alumina (Al2O3), Silicon carbide (SiC), Magnesium Oxide (MgO), Titanium diboride (TiB_2) and Aluminium (Al6061) were subjected to experimentation. To determine which parameters exert the most significant influence, three experiments were

carried out for each sample obtained from nine specimens, incorporating varying parameters. The objective of the experiment was to examine the influence of four parameters—Weight Percentage of Reinforcement, Speed (m/s), Load (N), and Distance (m)—on the wear loss of bio-ceramic composites. The findings of a wear analysis performed utilizing Design of Experiments (DOE) with an L27 Orthogonal array. The results of the experiment are presented in Figure 8, which shows the wear loss values for each 27 experiments [15].

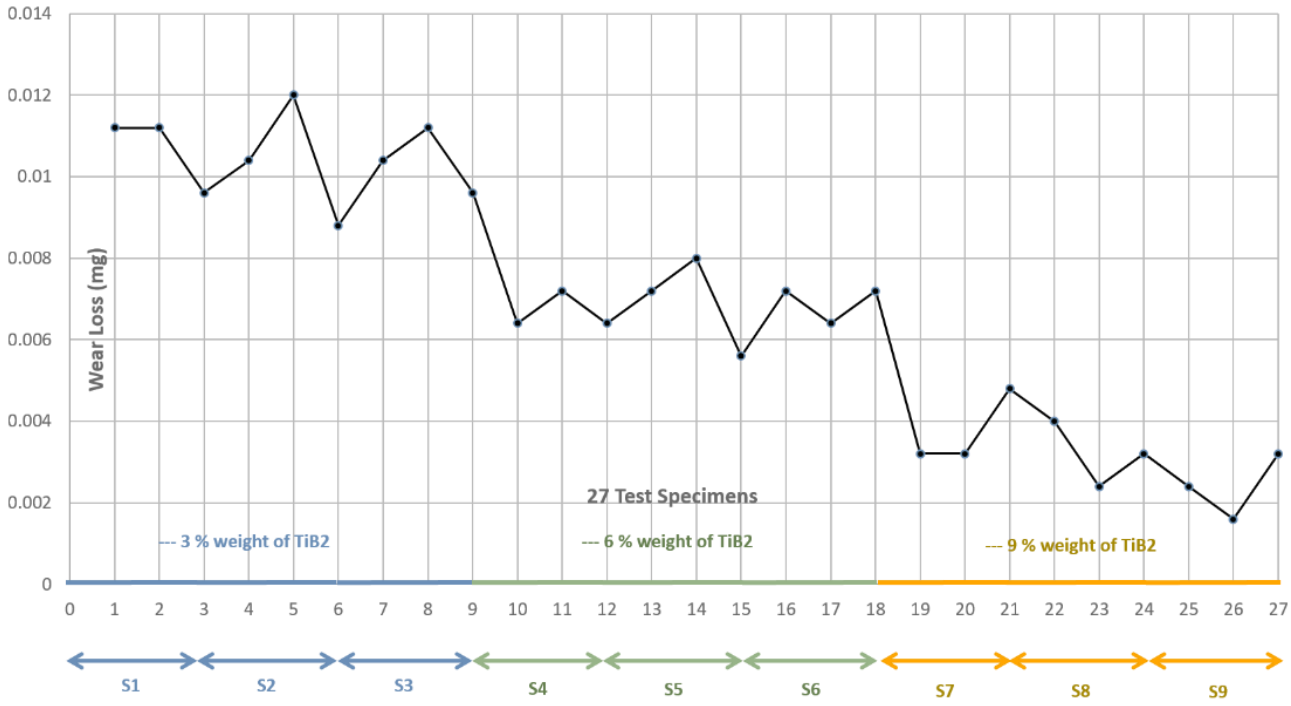

Fig 8. Experimental results for 27 test samples

The analysis of the test results was performed using Minitab software, the obtained S-N ratio values, response tables and the corresponding graphs were directly taken from Minitab software and are presented here. The specimens after the test were also subjected to SEM Analysis.

3.4 Model summary

The summary of the model demonstrates an excellent fit, confirmed by an R-Squared value of 89.21% and an adjusted R-Squared value of 84.42%. This indicates that the model accounts for a considerable portion of the variation observed in the wear loss data.

3.5 Analysis of variance (ANOVA)

The ANOVA table offers valuable insights regarding the significance of each parameter in relation to wear loss. The p-values indicate the probability of observing the test statistic under the null hypothesis that the parameter has no effect on the wear loss. The analysis confirms that the weight percentage of reinforcement is the most significant factor (p-value = 0.000), contributing 85.83% of the total variation, which highlights its dominant role in influencing tribological performance. This strong influence is consistent with TiB_2's high hardness (~30 GPa) and thermal stability, which reduce material removal during sliding wear.

Other factors, such as speed (0.68%, p-value = 0.440), load (1.12%, p-value = 0.470), and distance (1.57%, p-value = 0.294), have relatively minor contributions, indicating they have limited influence on wear loss under the tested conditions. These findings align with existing literature, where similar studies on Al-TiB_2 composites report reinforcement weight as the key factor affecting wear performance due to improved load transfer and grain refinement mechanisms. The residual error accounts for 10.79%, suggesting some unexplained variability, which could be attributed to experimental noise or untested factors.

Table 3 provides a clear quantitative understanding of the relative importance of each

parameter, aligning with the reviewer's request for highlighting effect sizes (% contributions). The statistical findings are further validated by comparing S-N ratio trends (Figure 9) with previous studies on ceramic-reinforced composites, which confirm that higher reinforcement levels significantly improve wear resistance through enhanced interfacial bonding and reduced abrasive wear [16]. Weight % of reinforcement exhibits the highest influence (Δ = 11.28), significantly improving wear resistance with higher levels. Speed (Δ = 0.96) shows negligible effect, while Load (Δ = 1.30) and Distance (Δ = 2.27) have moderate impacts, reinforcing the dominance of reinforcement weight in wear performance optimization.

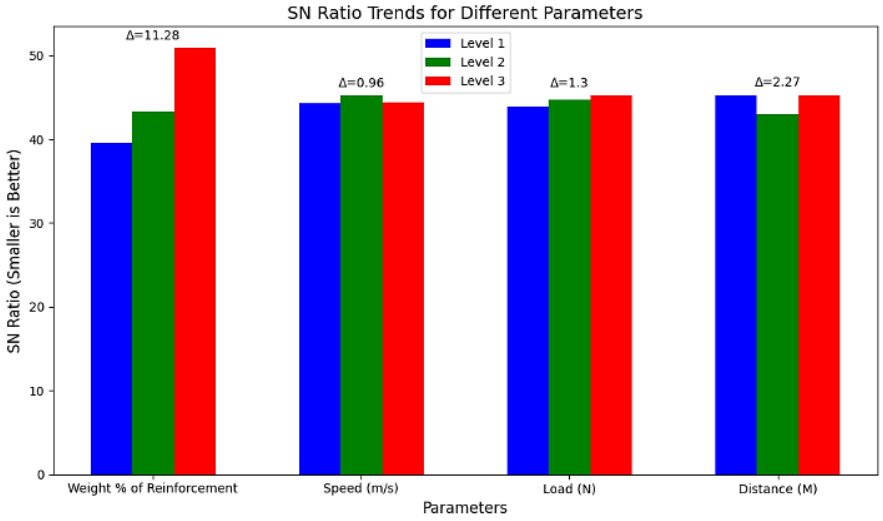

Fig 9. S-N ratio trends for different parameters.

Table 4. Analysis of Variance for S-N ratios.

Source	DF	Seq SS	Adj SS	Adj MS	F	P	**% Contribution/ Effect**
Weight % of Reinforcement	2	595.252	572.133	286.067	68.84	0.000	**85.83%**
Speed (m/s)	2	4.746	7.141	3.571	0.86	0.440	**0.68%**
Load (N)	2	7.794	6.548	3.274	0.79	0.470	**1.12%**
Distance (M)	2	10.899	10.899	5.449	1.31	0.294	**1.57%**
Residual Error	18	74.800	74.800	4.156			**10.79%**
Total	26	693.491					**100%**

Table 5. Response table for S-N Ratios (Fig. 9).

Level	Weight % of Reinforcement	Speed (m/s)	Load (N)	Distance (M)
1	39.62	44.24	43.91	45.29
2	43.34	45.21	44.75	43.03
3	50.91	44.42	45.20	45.29
Delta	11.28	0.96	1.30	2.27
Rank	1	4	3	2

Table 6. Response table for means.

Level	Weight % of Reinforcement	Speed (m/s)	Load (N)	Distance (M)
1	0.01048	0.00693	0.00702	0.0064
2	0.00684	0.00693	0.00675	0.0077
3	0.00302	0.00648	0.00657	0.0064
Delta	0.00746	0.00044	0.00044	0.0013
Rank	1	4	3	2

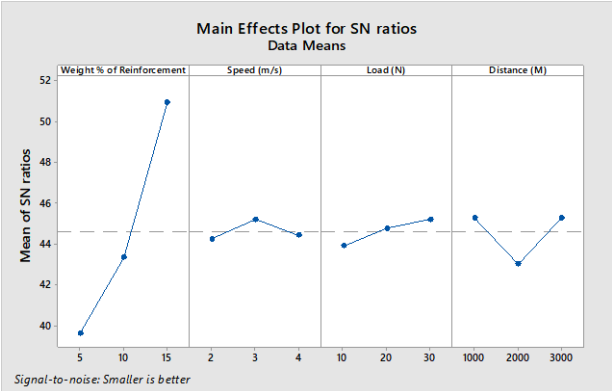

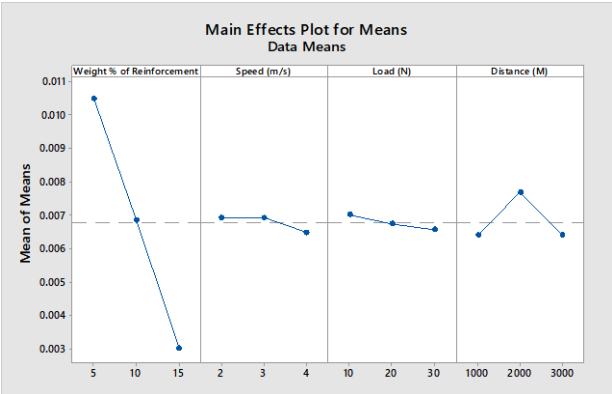

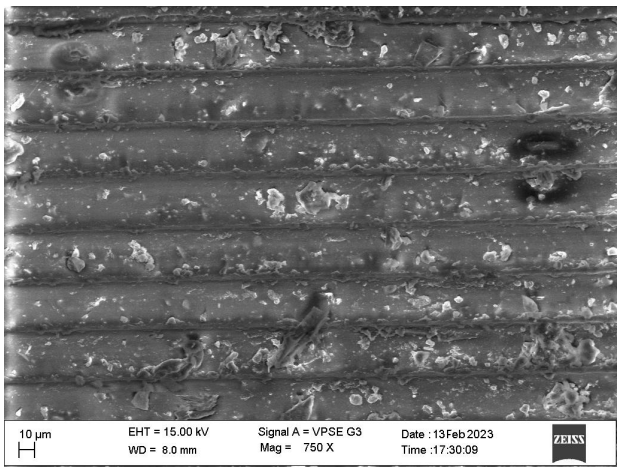

Sample with 3 % TiB_2

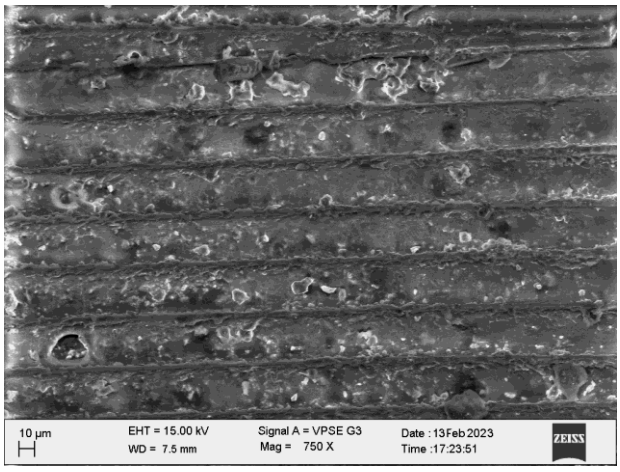

Sample with 6% TiB_2

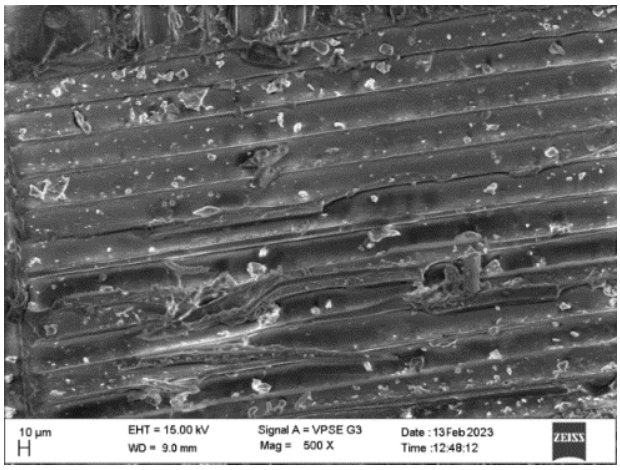

Sample with 9 % TiB_2

Figure 10. SEM analysis post wear test.

3.6 Scanning electron microscope images analysis

SEM images (Figure 10) reveal that the incorporation of higher TiB_2 content significantly reduces wear tracks due to its exceptional hardness (~30 GPa) and ability to resist material removal during sliding contact. This improvement is attributed to TiB_2's role in grain refinement, load transfer efficiency, and thermal stability, which enhance overall wear resistance. Microstructural characterization further highlights the densification behavior achieved through the Spark Plasma Sintering (SPS) process, where localized heating ensures uniform particle bonding and reduced porosity. The as-developed composite morphology exhibits a homogeneous distribution of reinforcing phases (TiB_2, SiC, MgO, Al_2O_3) within the Al6061 matrix, contributing to enhanced mechanical strength and wear resistance. However, minor micro-cracks were observed in samples with 9% TiB_2, indicating a trade-off between increased wear resistance and brittleness at higher reinforcement levels.

3.7 Factors contributing to enhanced performance

The enhanced wear resistance is primarily due to TiB_2's high hardness and fracture toughness, which resist abrasive forces during sliding. Additionally, TiB_2's interaction with Al6061 improves load transfer efficiency, while its thermal stability minimizes deformation under high temperatures.

Other reinforcements also contribute:

Al_2O_3 provides hardness and thermal stability but may increase brittleness at higher concentrations.

SiC enhances wear resistance through its high hardness (~9 Mohs) and acts as a load-bearing phase 6.

MgO improves grain refinement and mechanical properties but has limited direct impact on wear resistance.

Also, optimized composite (9% TiB_2) shows superior wear resistance compared to commercial hip implant materials like CoCr alloys and UHMWPE. For instance, CoCrMo alloys exhibit wear rates of ~0.76 mm^3/million cycles under similar conditions, whereas the current composite demonstrates significantly lower wear loss due to its ceramic reinforcement matrix.

In comparison with other studies on Al-TiB_2 composites:

- TiB_2-reinforced Al1050 composites fabricated via liquid pressing infiltration showed similar improvements in hardness and wear resistance but lacked biocompatibility testing [17].
- AA6061/TiC composites demonstrated a linear reduction in wear rate with increased reinforcement but were limited by adhesive wear mechanisms [18].

4. CONCLUSIONS

This study successfully fabricated advanced bioceramic composites specifically designed for use in Total Hip Arthroplasty, with a focus on enhancing the performance of hip implants.

- The Spark Plasma Sintering (SPS) process proved to be an effective method for the fabrication of these composites, resulting in materials with improved mechanical properties.
- Energy Dispersive Spectrum (EDS) analysis confirmed that aluminum serves as the base alloy in the composites, while reinforcing elements such as titanium, magnesium, boron, and silicon were also identified, contributing to the composite's overall performance.
- X-ray Diffraction (XRD) patterns validated the presence of TiB_2 particles, with distinct peaks indicating their crystalline structure, thereby confirming the integrity of the material across varying TiB_2 weight percentages.
- The L27 orthogonal array was effectively utilized in the experimental design, demonstrating its suitability for analyzing the influence of different parameters on the composite's performance.
- Through the Design of Experiments (DOE) approach, the effect of TiB_2 on the composite's tribological behavior was systematically evaluated. The analysis revealed that the weight percentage of TiB_2 is the most significant parameter affecting wear resistance, with a delta value of 11.28 and a p-value of 0.000.
- Scanning Electron Microscopy (SEM) images illustrated a trend of reduced wear tracks with increasing TiB_2 percentages, indicating that the incorporation of ceramics significantly enhances wear resistance. This finding underscores the importance of carefully considering the selection and design of composite materials for wear applications in hip implants.
- Overall, the optimal composition identified—comprising 5% alumina, 5% SiC, 2% MgO, and 9% TiB_2 combined with Al6061—demonstrated superior toughness and fracture resistance, addressing the fragility often associated with ceramic materials and highlighting its potential for long-term effectiveness in hip joint replacements.
- Comparing the advanced materials available in market, the optimized Al6061-TiB_2 composite demonstrates superior wear resistance compared to CoCrMo alloys and UHMWPE. The wear rate of CoCrMo alloys (~0.76 mm^3/million cycles) and UHMWPE liners is higher than that of TiB_2-reinforced composites due to TiB_2's exceptional hardness (~30 GPa) and thermal stability. Additionally, TiB_2 improves fracture toughness, addressing brittleness concerns associated with ceramic materials [19].
- Future studies will focus on advanced mechanical and tribological characterizations, including COF vs. time/load, fatigue behavior, and bio

tribological testing under simulated physiological conditions to further validate the composite's suitability for orthopaedic applications. Additionally, in vitro biocompatibility assessments will be conducted to ensure clinical relevance.

REFERENCES

[1] D. Shekhawat, A. Singh, M. K. Banerjee, T. Singh, and A. Patnaik, "Bioceramic composites for orthopaedic applications: A comprehensive review of mechanical, biological, and microstructural properties," *Ceramics International*, vol. 47, no. 3, pp. 3013–3030, Sep. 2020, doi: 10.1016/j.ceramint.2020.09.214.

[2] E. M. Roos and N. K. Arden, "Strategies for the prevention of knee osteoarthritis," *Nature Reviews Rheumatology*, vol. 12, no. 2, pp. 92–101, Oct. 2015, doi: 10.1038/nrrheum.2015.135.

[3] K. Ren, A. Dusad, Y. Zhang, and D. Wang, "Therapeutic intervention for wear debris-induced aseptic implant loosening," *Acta Pharmaceutica Sinica B*, vol. 3, no. 2, pp. 76–85, Mar. 2013, doi: 10.1016/j.apsb.2013.02.005.

[4] A. H. Choi, "Biomaterials and Bioceramics—Part 1: Traditional, Natural, and Nano," in *Springer series in biomaterials science and engineering*, 2022, pp. 1–45, doi: 10.1007/978-981-16-7435-8_1.

[5] A. Sen et al., "Standards of mechanical, physical, chemical, and biological properties of bioceramics," in *CRC Press eBooks*, 2023, pp. 327–343, doi: 10.1201/9781003258353-18.

[6] F. Melo-Fonseca, G. Miranda, H. S. Domingues, I. M. Pinto, M. Gasik, and F. S. Silva, "Reengineering Bone-Implant interfaces for improved mechanotransduction and clinical outcomes," *Stem Cell Reviews and Reports*, vol. 16, no. 6, pp. 1121–1138, Aug. 2020, doi: 10.1007/s12015-020-10022-9.

[7] V. Thomas, S. A. Catledge, P. Baker, G. P. Siegal, and Y. K. Vohra, "Ceramic coatings in Load-Bearing articulating joint implants," in *Elsevier eBooks*, 2016, pp. 315–347, doi: 10.1016/b978-0-12-802792-9.00007-0.

[8] R. A. Al-Samarai and Y. Al-Douri, "Wear in metals," in *Materials horizons*, 2024, pp. 61–105, doi: 10.1007/978-981-97-1168-0_3.

[9] G. Mallesh, R. Pavankumar, V. G. P. Kumar, and L. L. Naik, "Synthesis and characterization of AL 7072-AL2O3 metal matrix composites," in *Lecture notes in mechanical engineering*, 2020, pp. 167–181, doi: 10.1007/978-981-15-4745-4_16.

[10] G. Shen, F. Fang, and C. Kang, "Tribological Performance of Bioimplants: A Comprehensive review," *Nanotechnology and Precision Engineering*, vol. 8, iss. 1, pp. 107-122, Jun. 2018, doi: 10.13494/j.npe.20180003.

[11] R. Khanna, "Advances in bearing materials for total artificial hip arthroplasty," in *Springer eBooks*, 2017, pp. 467–494, doi: 10.1007/978-3-319-73664-8_17.

[12] A. Verma, S. S. Chauhan, and S. P. Dwivedi, "Review paper on thermal expansion and tribological behavior of composite materials," *Materials Today Proceedings*, vol. 79, pp. 235–246, Nov. 2022, doi: 10.1016/j.matpr.2022.11.073.

[13] W. R. Matizamhuka, "Spark plasma sintering (SPS) - an advanced sintering technique for structural nanocomposite materials," *Journal of the Southern African Institute of Mining and Metallurgy*, vol. 116, no. 7, pp. 1171–1180, Jan. 2016, doi: 10.17159/2411-9717/2016/v116n12a12.

[14] D. Bellucci et al., "Bioglass and bioceramic composites processed by Spark Plasma Sintering (SPS): biological evaluation Versus SBF test," *Biomedical Glasses*, vol. 4, no. 1, pp. 21–31, Jan. 2018, doi: 10.1515/bglass-2018-0003.

[15] M. M. Khan, A. Dey, and M. I. Hajam, "Experimental investigation and optimization of dry sliding wear test parameters of aluminum based composites," *Silicon*, vol. 14, no. 8, pp. 4009–4026, Jun. 2021, doi: 10.1007/s12633-021-01158-5.

[16] K. K. Sriram, N. Radhika, M. Sam, and S. S, "Studies on adhesive wear characteristics of centrifugally cast functionally graded ceramic reinforced composite," *International Journal of Automotive and Mechanical Engineering*, vol. 17, no. 4, Dec. 2020, doi: 10.15282/ijame.17.4.2020.05.0625.

[17] S. Ko et al., "Fabrication of TiB2–Al1050 Composites with Improved Microstructural and Mechanical Properties by a Liquid Pressing Infiltration Process," *Materials*, vol. 13, no. 7, p. 1588, Mar. 2020, doi: 10.3390/ma13071588.

[18] D. S. Rao and N. Ramanaiah, "Evaluation of Wear and Corrosion Properties of AA6061/TiB2 Composites Produced by FSP Technique," *Journal of Minerals and Materials Characterization and Engineering*, vol. 05, no. 06, pp. 353–361, Jan. 2017, doi: 10.4236/jmmce.2017.56029.

[19] B. Kumar, S. Saleem, M. F. Wani, R. Sehgal, and S. Kumar, "Influence of Nano-Lubrication on tribological behavior of AZ91 magnesium alloy under fretting condition," *Tribology in Industry*, vol. 45, no. 3, pp. 375–386, Sep. 2023, doi: 10.24874/ti.1426.12.22.06.